

# NUMERICAL AND EXPERIMENTAL ANALYSIS OF VORTEX SHEDDING PHENOMENA AROUND A SET OF RECTANGULAR CYLINDERS IN TANDEM.

## **Campregher , Rubens**

Faculty of Mechanical Engineering, FEMEC  
Federal University of Uberlândia, UFU  
38400-902 – Uberlândia - Brazil  
[campregher@mecanica.ufu.br](mailto:campregher@mecanica.ufu.br)

## **Silveira Neto, Aristeu**

Federal University of Uberlândia, UFU  
[aristeus@mecanica.ufu.br](mailto:aristeus@mecanica.ufu.br)

## **Mansur, Sérgio S.**

### **Vieira, E.D.R**

### **Duarte , Mílvio**

Mechanical Engineering Department  
UNESP Câmpus Ilha Solteira  
15385-000 – Ilha Solteira - SP - Brazil  
[mansur@dem.feis.unesp.br](mailto:mansur@dem.feis.unesp.br)

**Abstract.** *The flow around arrangement of cylinders is commonly encountered in real engineering applications: set of industrial chimneys, of buildings, compact heat exchangers tube banks, etc. So, the understanding of the phenomena related to the flow evolving around cylinders is very important in order to save design time and costs. This paper performs a numerical and experimental simulation of the flow around an in-line arrangement of two, three, and four square cylinders, in comparison with rectangular cylinders of side factor three, five, and seven, respectively. The numerical approach was employed to capture the Strouhal number drop down, encountered in the water tunnel experimental tests. Frequency spectrum, vorticity contours and dye wash technique were employed to ensure a proper analysis of the physical phenomena. The numerical code as well as the mesh generator was developed in FORTRAN and has been designed to use the Finite Volume Method. Furthermore, a SIMPLEC algorithm was used in pressure-velocity coupling and the QUICK scheme in the advective terms discretisation.*

**Keywords.** *rectangular cylinders, numerical and experimental simulation, tandem, cylinders arrangement.*

## **1. Introduction**

Most of the works about cylinders arrangement found in literature, are devoted to cylinders of circular shape, see Gu & Sun (1998) and Luo *et al.* (1995). This popular form is used in tube banks of compact heat exchangers, cable bundlers, set of chimneys, etc. and is widely studied. By the other side, the flow around a single rectangular cylinder, despite of its simple geometry, can generate a very complex behavior. Furthermore, when more than one rectangular cylinder are placed close enough to have their flow structures influencing each other, one can expect some interesting phenomena (Campregher *et al.*, 2001).

In this work, the Strouhal number drop down phenomenon, observed in the wake of a square cylinders in-line arrangement, is compared with the Strouhal number of a single rectangular cylinder having an equivalent length. Let the square cylinders dimension be named as B. Also, let the rectangular cylinders have the thickness B and the length (larger than its thickness) A, as illustrated in Fig. (1). The equivalent length is understood as the sum of the square cylinders dimensions and the space among them when compared with the single rectangular cylinder length. As an example, when three square cylinders (BxB dimensions) are placed in a in-line (tandem) arrangement, separated by B, one can state that its equivalent length is of a rectangular cylinder having a length dimension five times B. The length to thickness ratio is known as size factor ( $\phi$ ), defined by the Equation (1).

Having stated this definitions, the tests were performed, experimentally and numerically, at several Reynolds numbers, from 100 to 500, for three different geometric configurations: two square cylinders compared with a  $\phi = 3$  rectangular cylinder; three square cylinders compared with a  $\phi = 5$  rectangular cylinder, and four square cylinders compared with a  $\phi = 7$  rectangular cylinder. In the Fig. (1), one can see a picture representing the latter case, which allows defining some interesting and useful non-dimensional parameters:

side factor: 
$$\phi = \frac{A}{B}, \quad (1)$$

the Reynolds number: 
$$\text{Re} = \frac{\rho U_{\infty} B}{\mu}, \quad (2)$$

and the Strouhal number:

$$St = \frac{f B}{U_\infty}, \quad (3)$$

where  $\rho$  and  $\mu$  is the fluid density and dynamic viscosity, respectively, and  $U_\infty$  is the mean flow velocity. This fluid and flow characteristics are represented in the Reynolds number ( $Re$ ). It is well known that above a specific  $Re$  number, some vortices are shed, alternately, from both sides of the cylinder. The vortex shedding frequency is represented by  $f$ , and is related to the body characteristic length and the flow velocity by the Strouhal number ( $St$ ).

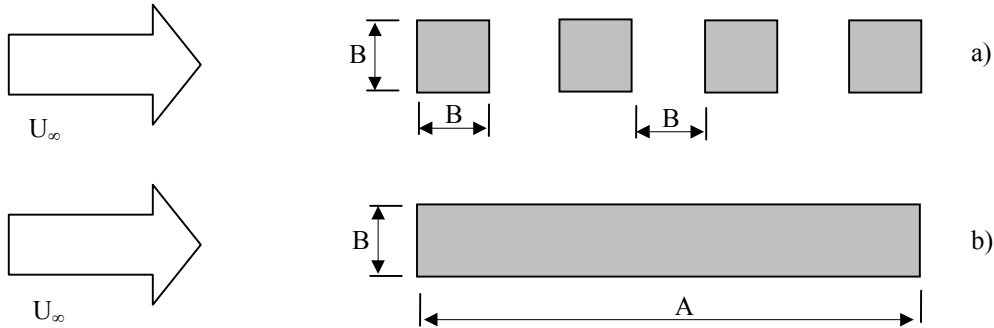


Figure 1. Four square cylinders in a tandem arrangement (a); and a  $\phi = 7$  rectangular cylinder (b).

## 2. Experimental apparatus

The experimental tests were performed in a low turbulence hydrodynamic tunnel driven by the action of the gravity. The tunnel test section is 146x146x500 mm, and is depicted in Fig.(2). This device is designed to operate both in continuous or in blow-down modes, as detailed by Vieira (1997). The vortex street visualization procedures were done by the dye wash technique. The dye, a mix of PVA pigments, ethylic alcohol, and water was injected into the stream by a 0.7mm diameter needle. The images were shot by a Nikon F4s SLR photo camera, having a 60mm/f.1:2,8 objective and recorded by a JVC video camera, model KY27CU, having three 2/3 inch 410.000 pixels CCD (*Charge-Coupled Devices*), of 800 lines of horizontal resolution and 63db of SNR (Signal Noise Ratio).

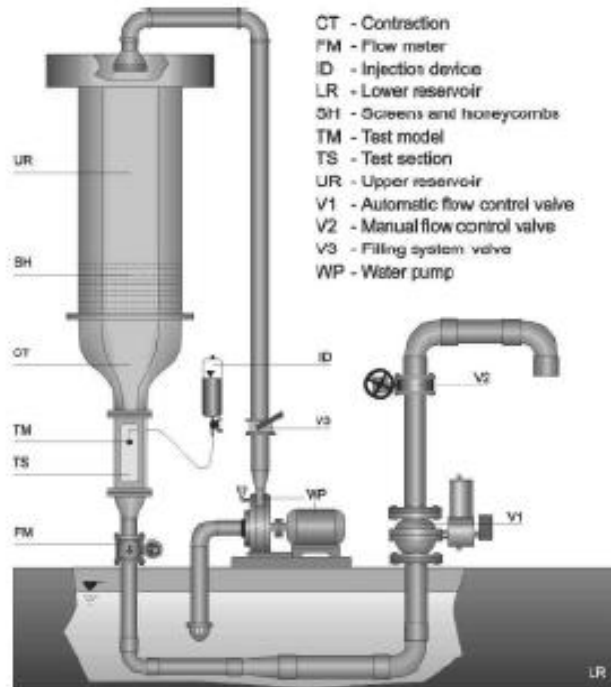


Figure 2. Low turbulence hydrodynamic tunnel.

The vortex shedding frequency was evaluated by the photograms counting technique, aided by a JVC video recorder, model BR-5822U, having TC (Time Code), TBC (Time Base Corrector), and DNR devices. The Time Code device generates a magnetic mark that allows tracking properly each photogram. So, the vortex shedding frequency is given by the fairly simple Equation below:

$$f = \frac{N F}{(I_N - I_0)}, \quad (4)$$

where  $N$  is the number of photograms on only one side of the body,  $F$  is the number of photograms per second, and  $I_N$  and  $I_0$  is the last and the first photograms, respectively, which identification is given by the TC device.

### 2.1. Test bodies

Several aluminum test bodies were machined and polished in a square and rectangular cross section shape. The drawing depicted in Fig. (3) represents the geometry pattern used, where  $B = 3\text{mm}$ ,  $C = 147.2\text{mm}$ , and  $A$  vary accordingly to the side factor ( $\phi$ ).

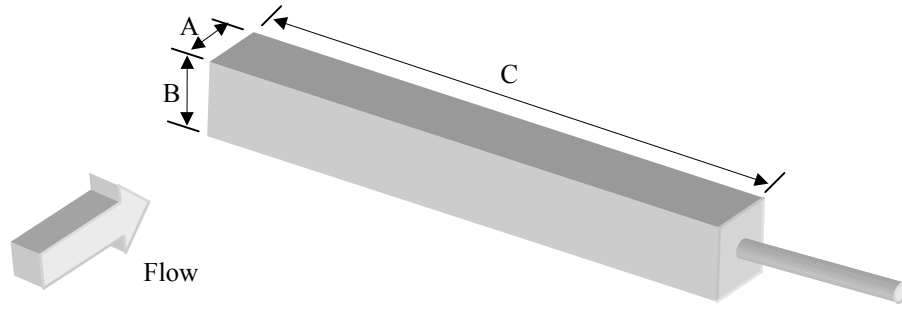


Figure 3. Test body dimensions.

### 3. Numerical modeling

An unsteady, incompressible, and isothermal flow of a Newtonian fluid can be modeled fairly good by the solution of the Navier-Stokes equations associated with the continuity equation. These equations are stated, respectively, as follows:

$$\frac{\partial}{\partial t} (u_i) + \frac{\partial}{\partial x_j} (u_i u_j) = -\frac{1}{\rho} \frac{\partial p}{\partial x_i} + \frac{\partial}{\partial x_j} \left( \nu \frac{\partial u_i}{\partial x_j} \right) + S c_i, \quad (5)$$

$$\frac{\partial}{\partial x_j} (u_j) = 0. \quad (6)$$

In this work, a two dimensional domain were employed. The domain was discretised by a non-uniform regular orthogonal mesh in order to obtain a higher density grid distribution over the bodies region. The advective terms were discretised by QUICK scheme (Hayase *et al.*, 1992) and the pressure-velocity coupling done by SIMPLEC algorithm (Patankar, 1980). A TDMA algorithm was employed to solve the velocity and pressure linear system. Due to the low Reynolds number flow regime, no turbulence modeling were used. The computational mesh designed for four square cylinders configuration is depicted in Fig. (4) and the numerical domain is detailed in Fig. (5).

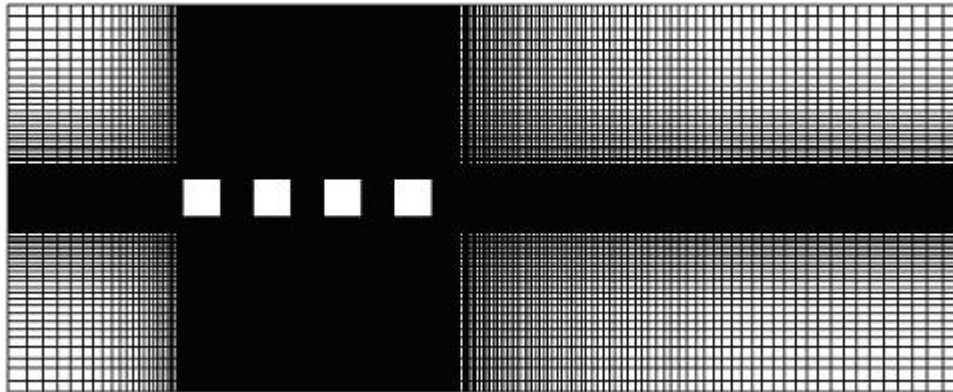


Figure 4. Computational mesh (410 x 120) for four square cylinders separated by  $B$ .

The numerical probes were placed 1.5B downstream the last cylinder. In the y direction, from bottom to top, the first probe was placed 1.5B below the domain centerline, the second one over the centerline, and the third one 1.5B above the centerline, as can be seen in the Fig. (5).

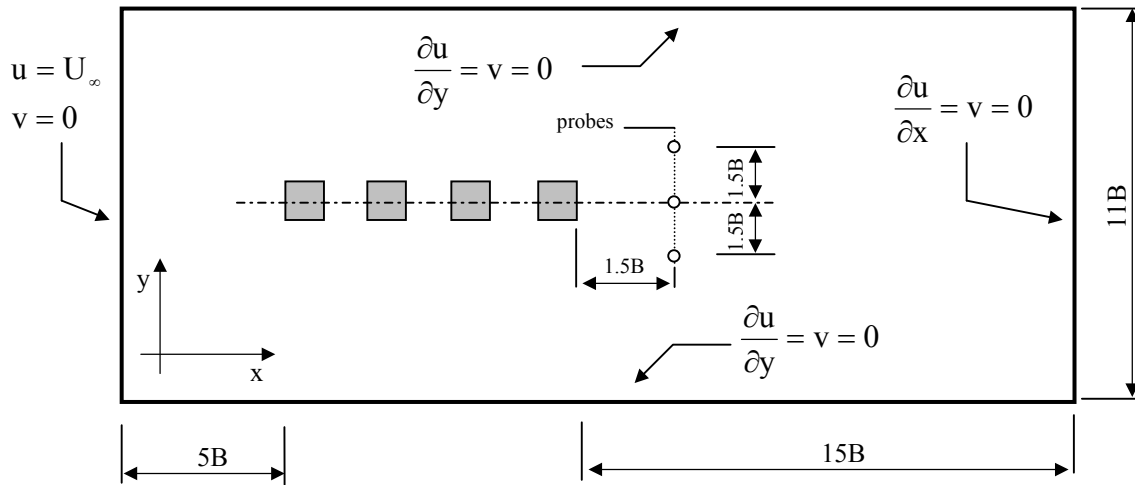


Figure 5. Detailed view of the computational domain.

#### 4. Results and discussion

The tests had been divided in three different geometric set: two square cylinders against one three side factor rectangular cylinder; three square cylinders against a five side factor rectangular cylinder; and four square cylinders against a seven side factor rectangular cylinder. Every one of these set were run in the hydrodynamic tunnel and numerically simulated.

##### 4.1. Arrangement of two square cylinders and an isolated rectangular cylinder with $\phi = 3$ .

The Reynolds numbers were varied from 108 to 500 in both experimental and numerical simulations. The results for main frequency and Strouhal numbers are summed up in the Tab. (1) and depicted in Fig. (7). No Strouhal number drop down was found in the tests with two square cylinders neither meaningful difference was noted between them and the size factor 3 rectangular cylinder, as can be seen in the pictures and graphics presented in the Fig. (6).

Table 1. Numerical and experimental results for Strouhal number in the first configuration.

Reynolds number	Two square cylinders - Strouhal (St)		$\phi = 3$ rectangular cylinder - Strouhal (St)	
	Experimental	Numerical	Experimental	Numerical
108	0,13	0,132	0,14	0,138
150	0,15	0,142	0,16	0,150
190	0,17	0,148	0,17	0,155
250	0,18	0,157	0,17	0,157
308	0,19	0,155	0,18	0,152
350	0,19	0,156	--	0,155
400	0,19	0,159	0,18	0,153
450	0,19	0,160	--	0,157
500	0,20	0,160	0,18	0,156

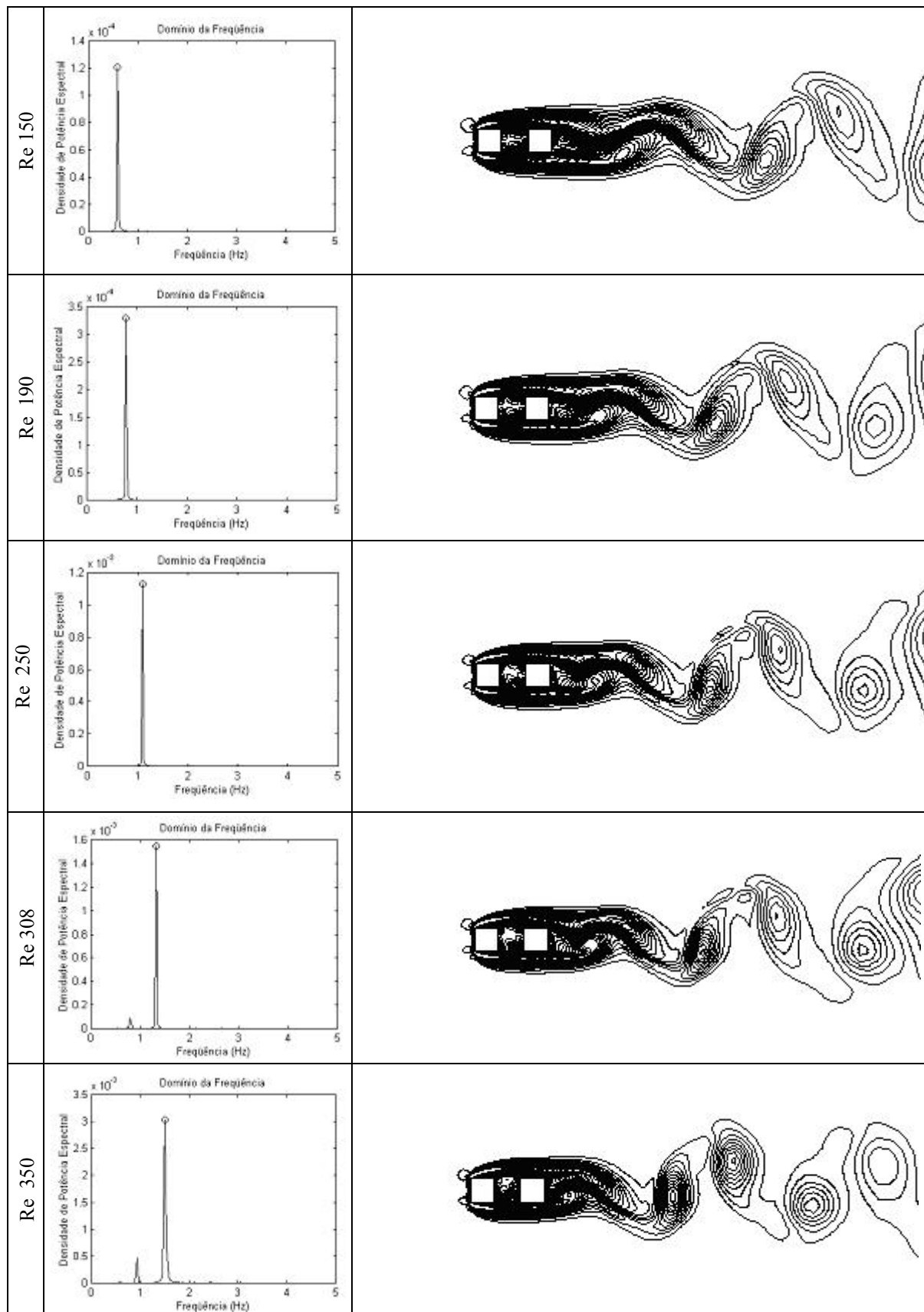


Figure 6. Vortex shedding frequency behavior for two square cylinders.

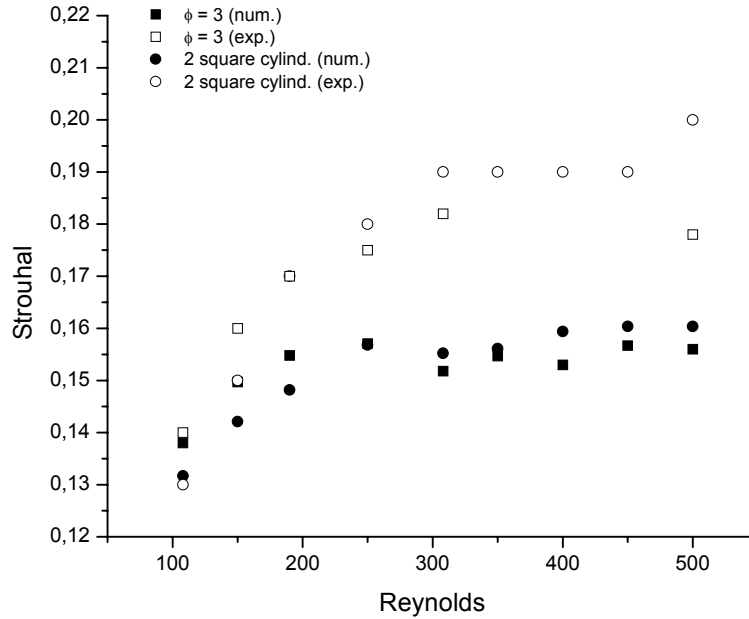


Figure 7. Strouhal number x Re number for the first configuration set of cylinders: two square cylinders compared with an isolated cylinder with  $\phi = 3$ .

#### 4.2. Arrangement of three square cylinders and an isolated rectangular cylinder with $\phi = 5$ .

Due to the drop down phenomenon observed in the three cylinders configuration, several intermediate tests were needed in order to get the transition effect in more details. The results for Strouhal numbers are displayed in Tab.(3). In the pictures in Fig. (8), it is possible to observe that the vortex shedding behind the last cylinder for  $Re = 281$  is more elongated than for  $Re = 228$ . This behavior could be related to a stronger interaction between the vortex shed behind the last cylinder and the ILEV (Impinging Shear Layer Vortex) around the cylinders. Such interaction tends to avoid the vortex generation just behind the last cylinder, and decreasing the shedding frequency. Consequently, decreasing the Strouhal number. One can see that the transition point, namely, the point where the interference of the ILEV become stronger, could be located at a critical Re number in somewhere between  $Re = 257$  and  $Re = 271$ .

The vortex shedding frequency graphs are depicted in Fig. (9) left column. It is also presented the corresponding vorticity contours on right column, where its possible to recognize the inversion at the main vortex frequency, from a higher value to a lower one in somewhere around the critical Re number.

Table 3. Numerical and experimental results for Strouhal number in the second configuration.

Reynolds number	Three square cylinders - Strouhal (St)		$\phi = 5$ rectangular cylinder - Strouhal (St)	
	Experimental	Numerical	Experimental	Numerical
108	0,12	0,119	0,12	0,128
150	0,14	0,136	0,14	0,141
190	0,16	0,146	0,16	0,150
228	0,16	0,150	--	--
257	0,16	0,153	0,17	0,159
271	0,10	0,086	--	--
281	0,11	0,087	--	--
308	0,10	0,084	0,18	0,162
350	--	--	0,21	0,162
400	0,10	0,089	0,26	0,196
413	0,10	0,087	--	--
450	--	--	--	0,155
463	0,11	0,098	--	--
500	--	0,088	--	0,156

### 4.3. Arrangement of four square cylinders and an isolated rectangular cylinder with $\phi = 7$ .

In the four square cylinders configuration, the Strouhal number drop down phenomenon was also observed, as can be seen in the Fig. (10) left column graphs. Once again, the wake elongation process, visualized in three cylinders tests was reproduced, and is depicted in the Fig. (10) right column. This behavior has, apparently, influence over the Strouhal number, as noted in the previous configuration and not realized in the first one, as can be seen in Fig. (11). Is worth noting that the flow recirculation becoming stronger from the first two cylinders gap to the last two gaps. Such recirculation could influence the regular vortex shedding pattern, giving some contribution to the Strouhal number drop down.

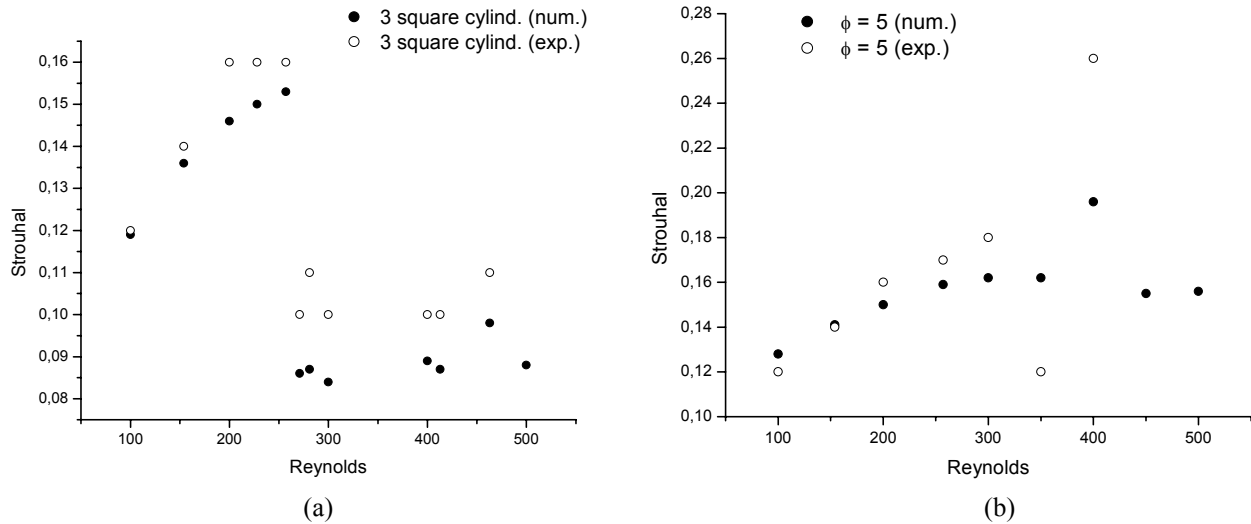


Figure 8. Strouhal number x Re number for the first configuration set of cylinders: three square cylinders (a) compared with an isolated cylinder with  $\phi = 5$  (b).

Table 4. Numerical and experimental results for Strouhal number in the third configuration.

Reynolds number	Four square cylinders - Strouhal (St)		$\phi = 7$ rectangular cylinder - Strouhal (St)	
	Experimental	Numerical	Experimental	Numerical
108	0,12	0,118	0,11	0,138
150	0,13	0,134	0,13	0,150
190	0,15	0,141	0,15	0,155
220	---	0,147	---	---
230	---	0,150	---	---
240	---	0,083	---	---
250	0,16	0,080	0,16	0,157
260	---	0,082	---	---
270	---	0,082	---	---
280	---	0,083	---	---
290	---	0,085	---	---
308	0,17	0,085	0,10	0,152
350	0,18	0,088	0,10	0,155
400	0,17	0,088	0,10	0,153
450	0,16	0,088	0,11	0,157
500	0,17	0,089	0,10	0,156

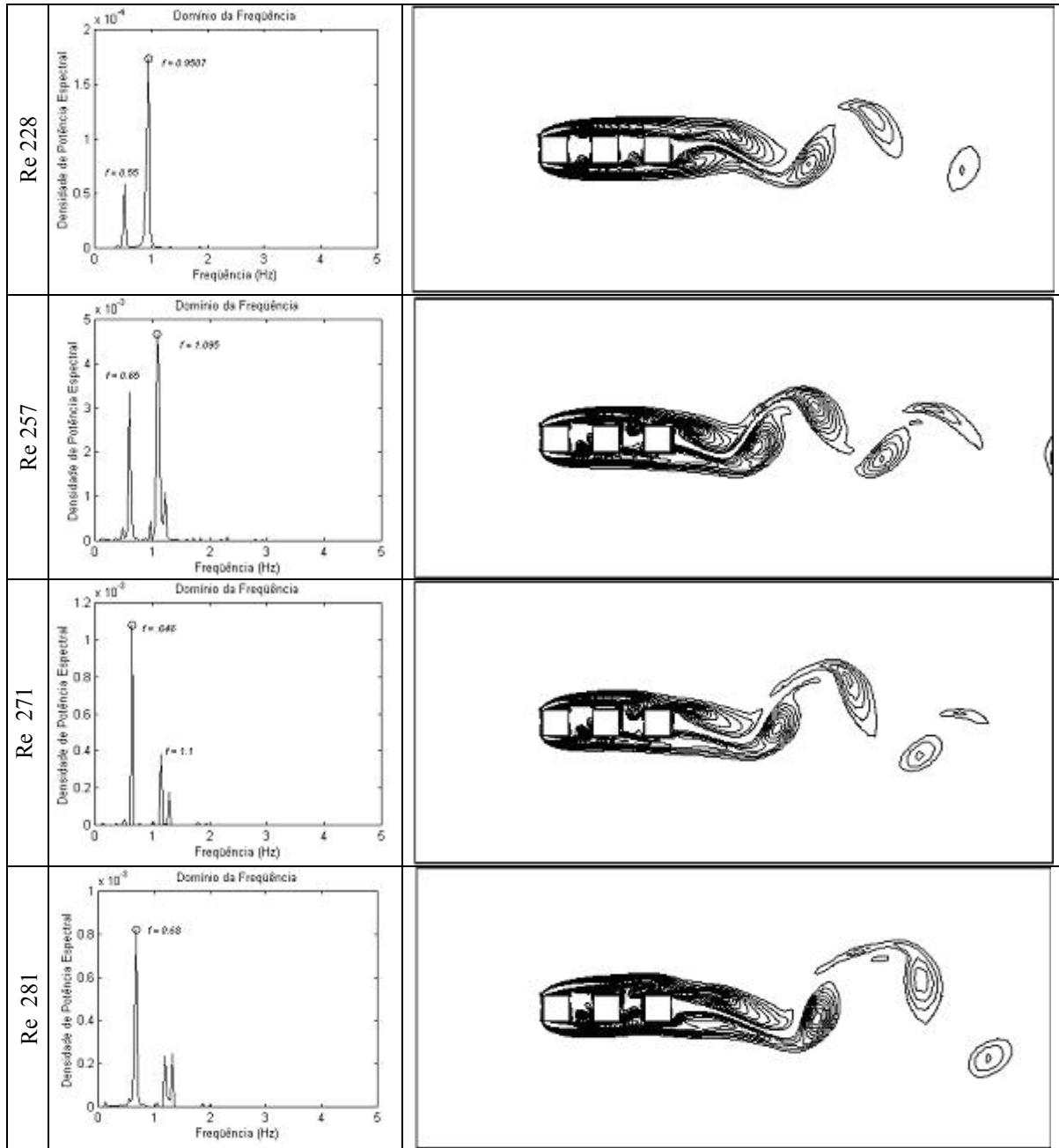


Figure 9. Vortex shedding frequency behavior for three square cylinders.

## 5. Conclusions

Is interesting to note that the discontinuity in the Strouhal number observed in two of the geometric set of cylinders is also encountered in rectangular cylinders side factor experiments. Nakamura (1996) had run several experimental tests, reproduced numerically by Campregher (2002), where the Strouhal tends to increase in a non-continuous mode with the increase in the side factor value. In these tests, the ILEV and TEVS (Trailing Edge Vortex Shedding) interaction showed great importance in vortex shedding frequency. However, in this case, the ILEV were galloping on the cylinders sides and, when they met the Von Karman type TEVS, there were the interference which promoted the oscillations in the Strouhal number.

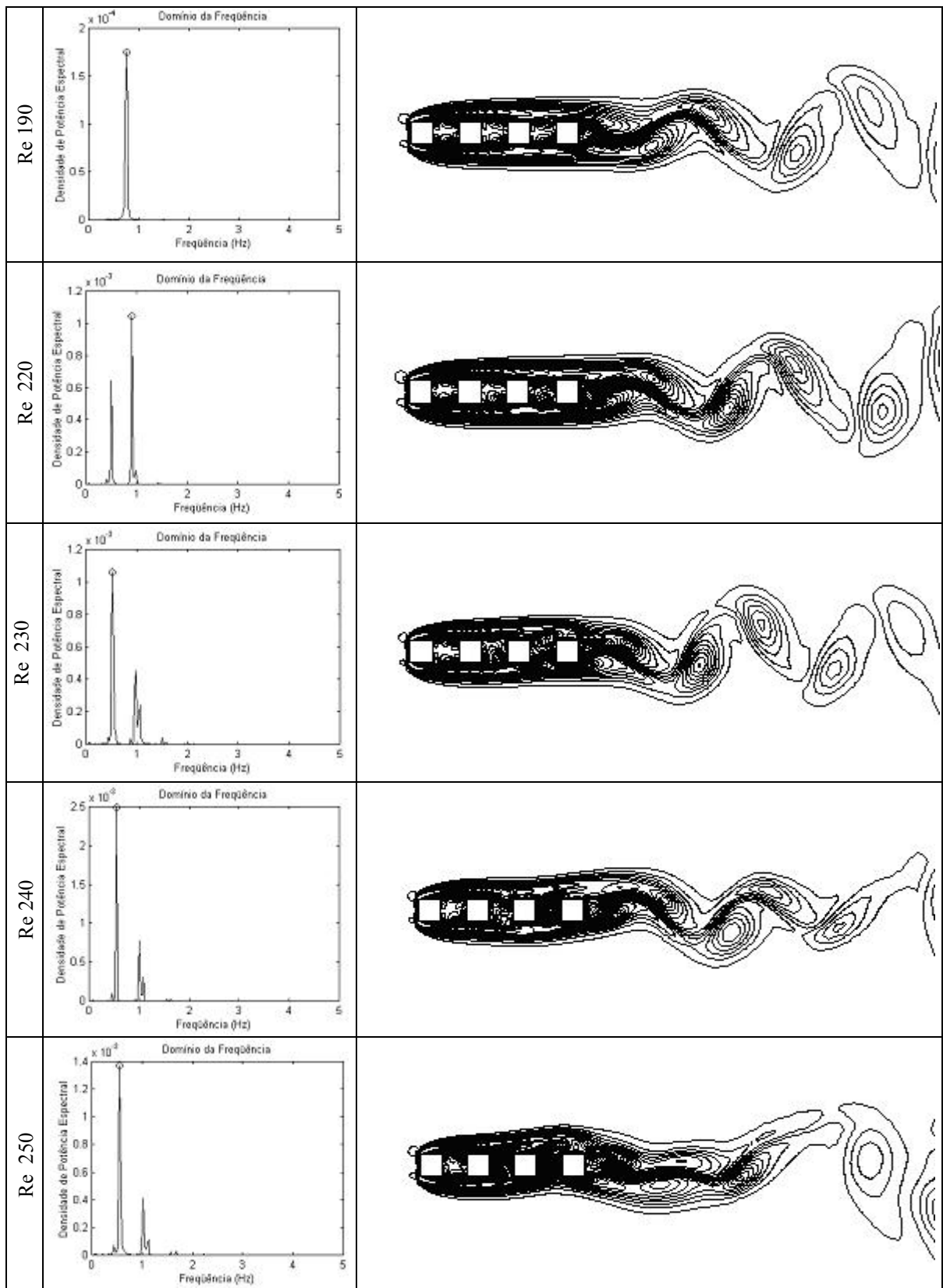


Figure 10. Vortex shedding frequency behavior for four square cylinders.

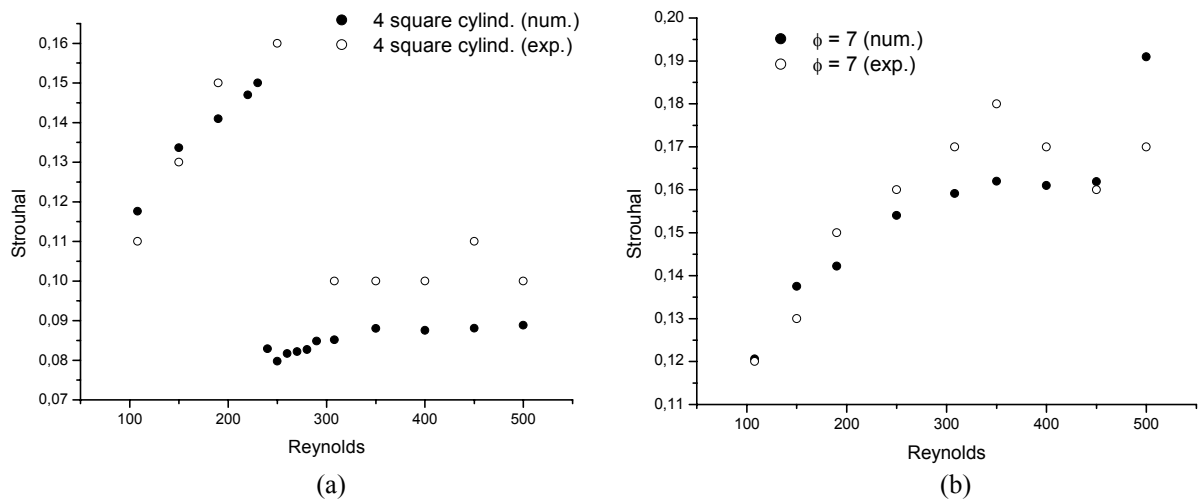


Figure 11. Strouhal number  $\times$  Re number for the first configuration set of cylinders: four square cylinders (a) compared with an isolated cylinder with  $\phi = 7$  (b).

In this work, the interference could be due the ILEV generated on the first cylinder front corner plus the vortex on the middle cylinder (in case of the three square cylinders) and on the two middle cylinders (in case of the four square cylinders configuration). This possibility is reinforced by the lack of Strouhal number drop down in the two square cylinders arrangement. Furthermore, this interference did not cause an oscillating Strouhal, but a lower and well-defined Strouhal number.

The fact of the Strouhal number, after its drop down, was kept constant in a fairly wide range of Reynolds numbers, suggest that this interesting characteristic could be more explored when a regular vortex shedding is desired.

However, in order to ensure a more wide application, several additional tests with different gap distances, number of square cylinders, and Reynolds number would be needed.

## 6. References

- Campregher, R., 2002, “Simulação Numérica de Escoamentos Transicionais e Turbulentos ao Redor de Geometrias Cartesianas”, MSc. Thesis, UNESP - Ilha Solteira, SP, Brazil.
- Campregher, R., Almeida, O., Mansur, S.S., Vieira, E.D.R., Silveira-Neto, A., 2001, “Numerical and Experimental Analysis of the Vortex Shedding Around an Arrangement of Parallel Rectangular Cylinders in Cross-flow at Reynolds Numbers up to 1000”, Proceedings of the XVI Brazilian Congress of Mechanical Engineering, CD-ROM, Uberlândia, MG, Brazil.
- Gu, Z., Sun T., 1999, “On Interference Between Two Circular Cylinders in Staggered Arrangement at High Subcritical Reynolds Numbers”, Journal of Wind Engineering and Industrial Aerodynamics, vol. 80, pp.287-309.
- Hayase, T., Humphrey, J.A.C., Greif, R., 1992, “A Consistently Formulated QUICK Scheme for Fast and Stable Convergence Using Finite-Volume Iterative Calculation Procedures”, Journal of Computational Physics, vol. 98, p.018-118.
- Luo, S.C., Gan T.L., Chew, Y.T., 1996, “Uniform Flow Past One (or Two in Tandem) Finite Length Circular Cylinder(s)”, Journal of Wind Engineering and Industrial Aerodynamics, vol. 59, pp.69-93.
- Nakamura, Y., Ohya, Y., Ozono, S., Nakayama, R., 1996, “Experimental and Numerical Analysis of Vortex Shedding from Elongated Rectangular Cylinders at Low Reynolds Number 200 – 1000”, Journal of Wind Engineering and Industrial Aerodynamics, vol. 65, pp.301-308.
- Patankar, S.V., 1980, “Numerical Heat Transfer and Fluid Flow”, Hemisphere.
- Vieira, E.D.R., 1997, “Estudo Qualitativo e Quantitativo do Escoamento ao Redor de Corpos Não-Aerodinâmicos Utilizando Técnicas de Visualização em Meio Hidrodinâmico”, PhD Dissertation, Instituto Tecnológico de Aeronáutica – ITA, São José dos Campos, SP, Brazil.

## 7. Copyright Notice

The author is the only responsible for the printed material included in his paper.